

XXIV PHYSICS IN COLLISION - Boston, June 27-29, 2004

## DIFFRACTIVE SCATTERING

Halina Abramowicz

*Raymond and Beverly Sackler Faculty of Exact Sciences*

*School of Physics and Astronomy*

*Tel Aviv University, Tel Aviv, Israel*

### ABSTRACT

Recent experimental results on inclusive diffractive scattering and on exclusive vector meson production are reviewed. The dynamical picture of hard diffraction emerging in perturbative QCD is highlighted.

## 1 Introduction

In hadron-hadron scattering, interactions are classified by the characteristics of the final states. In elastic scattering, both hadrons emerge unscathed and no other particles are produced. In diffractive dissociation, the energy transfer between the two interacting hadrons remains small, but one (single dissociation) or both (double dissociation) hadrons dissociate into multi-particle final states, preserving the quantum numbers of the associated initial hadron. The remaining configurations correspond to inelastic interactions.

The most difficult conceptual aspect of diffractive scattering is to provide a unique and concise definition. This will not be attempted here and diffraction will be understood as an interaction between projectile and target that generates a large rapidity gap between the respective final states, which is not exponentially suppressed.

Diffractive interactions are mediated by the exchange of a colorless object, with quantum numbers of the vacuum. This definition fits very well the framework of soft interactions, where diffractive scattering is mediated by the exchange of the universal Pomeron trajectory ( $\mathbb{P}$ ), introduced by Gribov [1]. Ingelman and Schlein [2] proposed to use diffractive scattering in the presence of a large scale to establish the partonic content of the Pomeron.

In QCD, the candidate for vacuum exchange with properties similar to the soft Pomeron is two gluon exchange [3, 4]. As a result of interactions between the two gluons, a ladder structure develops. In perturbative QCD (pQCD), the properties of this ladder depend on the energy and scales involved in the interaction, implying its non-universal character.

Each of the approaches mentioned above leads to definite predictions, which can be tested in high energy diffractive interactions in the presence of a hard scale. This has been pursued in  $ep$  scattering at HERA and in  $p\bar{p}$  scattering at the Tevatron. The purpose of this talk is to summarize the recently achieved progress.

## 2 Kinematics of hard diffractive scattering

The variables used to analyze diffractive scattering will be introduced for deep inelastic  $ep$  scattering (DIS). Since DIS is perceived as a two-step process, in which the incoming lepton emits a photon which then interacts with the proton target, the relevant variables can be readily generalized to  $p\bar{p}$  interactions. A diagram for diffractive scattering in DIS, where the diffracted state is separated from the scat-

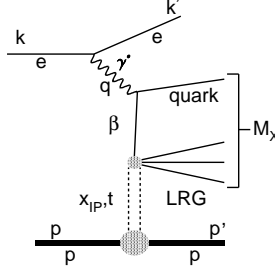


Figure 1: *Schematic diagram for diffractive DIS in ep interactions.*

tered proton by a large rapidity gap (LRG), is presented in figure 1 and all the relevant four vectors are defined therein. The usual DIS variables are the negative of the mass squared of the virtual photon,  $Q^2 = -q^2 = -(k - k')^2$ , the square of the center of mass energy of the  $\gamma^*p$  system,  $W^2 = (q + p)^2$ , the Bjorken scaling variable,  $x = \frac{Q^2}{2p \cdot q}$ , which in the Quark Parton Model constitutes the fraction of the proton momentum carried by the interacting quark, and the inelasticity,  $y = \frac{p \cdot q}{p \cdot k}$ . In addition to the usual DIS variables, the variables used to describe the diffractive final state are,

$$t = (p - p')^2, \quad (1)$$

$$x_P = \frac{q \cdot (p - p')}{q \cdot p} \simeq \frac{M_X^2 + Q^2}{W^2 + Q^2}, \quad (2)$$

$$\beta = \frac{Q^2}{2q \cdot (p - p')} = \frac{x}{x_P} \simeq \frac{Q^2}{Q^2 + M_X^2}. \quad (3)$$

$x_P$  is the fractional proton momentum which participates in the interaction with  $\gamma^*$ . It is sometimes denoted by  $\xi$ .  $\beta$  is the equivalent of Bjorken  $x$  but relative to the exchanged state.  $M_X$  is the invariant mass of the hadronic final state recoiling against the leading proton,  $M_X^2 = (q + p - p')^2$ . The approximate relations hold for small values of the four-momentum transfer squared  $t$  and large  $W$ , typical of high energy diffraction.

### 3 Formalism of diffractive scattering

To describe diffractive DIS, it is customary to choose the variables  $x_P$  and  $t$  in addition to the usual  $x$  and  $Q^2$  in the cross section formula. The diffractive contribution to  $F_2$  is denoted by  $F_2^D$  and the corresponding differential contribution, integrated over  $t$ , is

$$F_2^{D(3)} = \frac{dF_2^D}{dx_P}, \quad (4)$$

The three-fold differential cross section for  $ep$  scattering can be written as

$$\frac{d^3\sigma_{ep}^D}{dx_P dx dQ^2} = \frac{2\pi\alpha^2}{xQ^4} [1 + (1-y)^2] \sigma_r^{D(3)}(x, Q^2, x_P), \quad (5)$$

where

$$\sigma_r^{D(3)} = F_2^{D(3)} - \frac{y^2}{1 + (1-y)^2} F_L^{D(3)}. \quad (6)$$

$F_L^{D(3)}$  stands for the diffractive longitudinal structure function, which may not be small. The structure function  $F_2$  is related to the absorption cross section of a virtual photon by the proton,  $\sigma_{\gamma^*p}$ . For diffractive scattering, in the limit of high  $W$  (low  $x$ ),

$$F_2^{D(3)}(x, Q^2, x_P) = \frac{Q^2}{4\pi^2\alpha} \frac{d^2\sigma_{\gamma^*p}^D}{dx_P}. \quad (7)$$

This relation allows predictions for diffractive scattering in DIS based on Regge phenomenology applied to  $\gamma^*p$  scattering. In fact many of the questions that are addressed in analyzing diffractive scattering are inspired by Regge phenomenology as established in soft hadron-hadron interactions.

### 3.1 Regge phenomenology

The scattering of two hadrons,  $a$  and  $b$ , at squared center of mass energy  $s \gg m_{a,b}^2$ ,  $t$ , is described by the exchange of the universal  $\mathbb{P}$  trajectory parameterized as  $\alpha_P(t) = \alpha_P(0) + \alpha'_P t$ . The  $\mathbb{P}$  trajectory determines the  $s$  dependence of the total cross section,  $\sigma_{tot} \sim s^{\alpha_P(0)-1}$ . The ratio of elastic and diffractive to total cross sections, is expected to rise like  $s^{\alpha_P(0)-1}$ . A steep and universal  $x_P$  dependence of the diffractive cross section is expected,  $d\sigma^D/dx_P \sim x_P^{-(2\alpha_P(t)-1)}$ .

Values of  $\alpha_P(0) = 1.081$  [5] and  $\alpha'_P = 0.25 \text{ GeV}^{-2}$  [6] were derived based on total hadron-proton interaction cross sections and elastic proton-proton data. Recently the  $\mathbb{P}$  intercept has been reevaluated [7, 8] leading to a value of  $\alpha_P(0) = 1.096 \pm 0.03$ .

The positive value of  $\alpha'_P$  implies that the slope of the  $t$  distribution is increasing with  $\ln s$ . This fact, borne out by the hadron-hadron and photoproduction data (for a review and new data see [9]), is known as shrinkage of the  $t$  distribution. It is due to the fact that  $\alpha'_P > 0$  and has been explained by Gribov [1] as diffusion of particles in the exchange towards low transverse momenta,  $k_T$ , with  $\alpha'_P \sim 1/k_T^2$  (see also [10]).

### 3.2 QCD factorization and diffractive partons

QCD factorization for the diffractive structure function of the proton,  $F_2^D$ , is expected to hold [11, 12, 13], while it cannot be proven for hadron-hadron interactions [11].  $F_2^D$  is decomposed into diffractive parton distributions,  $f_i^D$ , in a way similar to the inclusive  $F_2$ ,

$$\frac{dF_2^D(x, Q^2, x_P, t)}{dx_P dt} = \sum_i \int_0^{x_P} dz \frac{df_i^D(z, \mu, x_P, t)}{dx_P dt} \hat{F}_{2,i}\left(\frac{x}{z}, Q^2, \mu\right), \quad (8)$$

where  $\hat{F}_{2,i}$  is the universal structure function for DIS on parton  $i$ ,  $\mu$  is the factorization scale at which  $f_i^D$  are probed and  $z$  is the fraction of momentum of the proton carried by the diffractive parton  $i$ . Diffractive partons are to be understood as those which lead to a diffractive final state. The DGLAP evolution equation applies in the same way as for the inclusive case. For a fixed value of  $x_P$ , the evolution in  $x$  and  $Q^2$  is equivalent to the evolution in  $\beta$  and  $Q^2$ .

If, following Ingelman and Schlein [2], one further assumes the validity of Regge factorization,  $F_2^D$  may be decomposed into a universal  $\mathbb{P}$  flux and the structure function of the  $\mathbb{P}$ ,

$$\frac{dF_2^D(x, Q^2, x_P, t)}{dx_P dt} = f_{\mathbb{P}/p}(x_P, t) F_2^{\mathbb{P}}(\beta, Q^2), \quad (9)$$

where the normalization of either of the two components is arbitrary. It implies that the  $x_P$  and  $t$  dependence of the diffractive cross section is universal, independent of  $Q^2$  and  $\beta$ , and given by

$$f_{\mathbb{P}/p}(x_P, t) \sim \left(\frac{1}{x_P}\right)^{2\alpha_{\mathbb{P}}(0)-1} e^{(b_0^D - 2\alpha'_{\mathbb{P}} \ln x_P)t}, \quad (10)$$

one of the expectations which is subject to experimental tests.

The mechanism for producing LRG is assumed to be present at some scale and the evolution formalism allows to probe the underlying partonic structure. The latter depends on the coupling of quarks and gluons to the Pomeron.

## 4 Measurements of $F_2^D$ at HERA

At HERA the diffractive candidate events are selected either by requiring a large rapidity gap [14, 15], or by requiring a leading proton [16]. The various analyses differ in the way the non-diffractive contributions are treated and in the way the proton dissociative events are subtracted. The comparison between the various

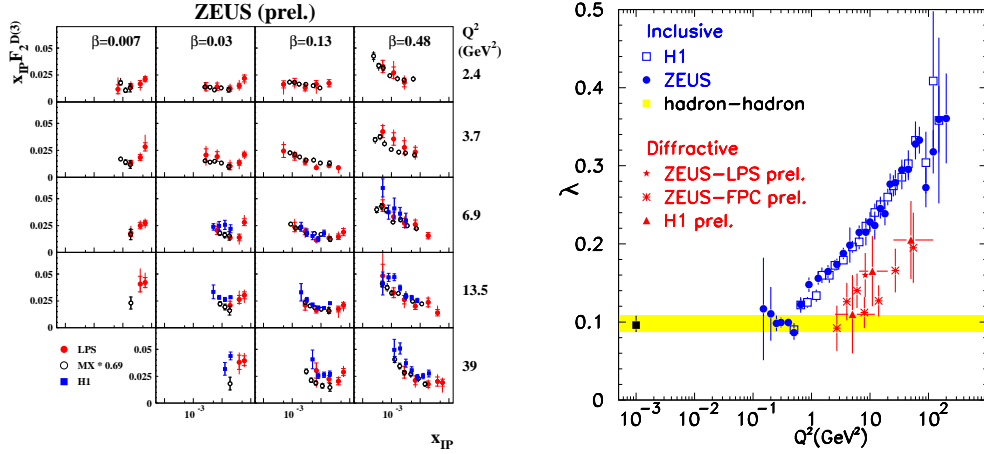


Figure 2: *Left: comparison of  $x_P F_2^{D(3)}$  measured by H1 [14] and ZEUS [16, 15] as a function of  $x_P$  in overlapping bins of  $\beta$  and  $Q^2$ . Right:  $Q^2$  dependence of  $\lambda = \alpha_P(0) - 1$  fitted to the measurements of  $F_2$  and  $F_2^D$  of the proton, as denoted in the figure.*

measurements is shown in figure 2. The  $x_P$  dependence of  $F_2^{D(3)}$ , in the region of  $x_P < 0.01$ , is expected to be dominated by  $\mathbb{P}$  exchange. The corresponding values of  $(\alpha_P(0) - 1)$  are shown as a function of  $Q^2$  in figure 2. A dependence of  $\alpha_P$  on  $Q^2$  cannot be excluded, however the errors are large enough, so that a constant value of  $\alpha_P(0)$  fits the data. However averaged over the whole  $Q^2$  range the value of  $\alpha_P$  is definitely larger than the intercept of the soft Pomeron. In addition, the diffractive  $\alpha_P(0) - 1$  value is only half of that for inclusive  $F_2$  measurements, also shown in the figure. This means that the ratio of diffractive to total  $\gamma^*p$  cross sections is constant with  $W$ . Those are indications that the connection of diffractive DIS to the simple soft  $\mathbb{P}$  picture is not straight forward.

#### 4.1 Diffractive parton distributions

The H1 measurements of  $F_2^{D(3)}$  [14], which cover by far the largest phase space, have been used to perform a QCD evolution fit to extract diffractive parton distribution functions (DPDF). The results of the fit are shown in figure 3. A very good description of the data is obtained, provided the parton distributions are dominated by gluons, which carry about 80% of the momentum of partons leading to diffractive events. This latest extraction of DPDFs by H1 is called H1 2002 DPDFs.

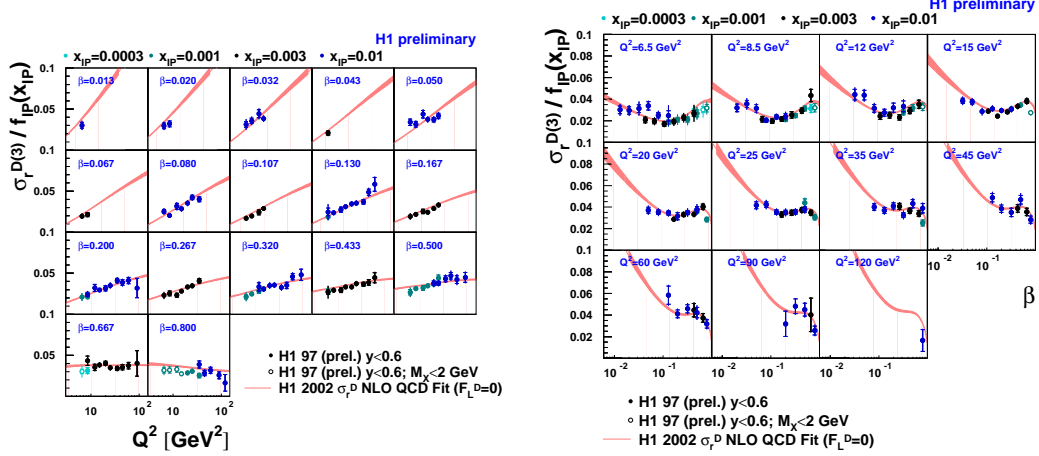


Figure 3: Comparison of NLO QCD fit with the measurements of  $\sigma_r^D$  after dividing out the flux term. Left, the scaling violation in bins of  $\beta$ ; right, the  $\beta$  distribution in bins of  $Q^2$ .

#### 4.2 Tests of QCD factorization

QCD factorization can be tested in high transverse momenta,  $p_T$ , jet production in  $\gamma^*p$ ,  $\gamma p$  and  $p\bar{p}$  diffractive production.

If factorization holds, the cross section for production of jets [17] and charm [18, 19] in  $\gamma^*p$  should be well reproduced by NLO calculations with DPDFs, extracted from structure function measurements. This is indeed the case as demonstrated in figure 4.

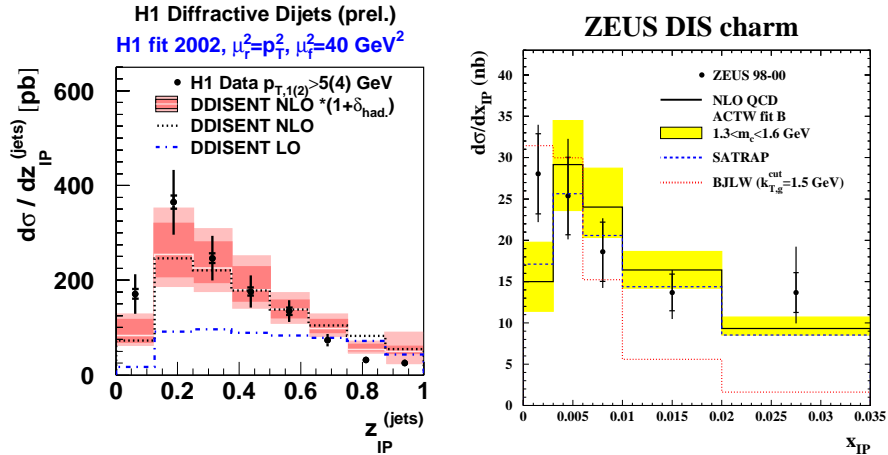


Figure 4: Left: distribution of  $z_{IP}^{jets}$ , the estimate of the diffractive parton momentum fraction of IP, for dijet production. Right: the  $x_{IP}$  distribution for diffractive events containing charm in the final state.

QCD factorization breaking is observed in hard diffractive scattering in  $p\bar{p}$ . Measurements [20] of two jet production accompanied by the presence of a leading anti-proton have been used to extract the effective diffractive structure function for two jet production  $F_{JJ}^D$ , which can then be compared with the expectations from DPDF extracted at HERA. As shown in figure 5, even for the H1 2002 DPDFs, where the abundance of gluons is lesser compared to earlier DPDFs [21], the expectations are by about a factor 10 above the measurements. It should be stressed however,

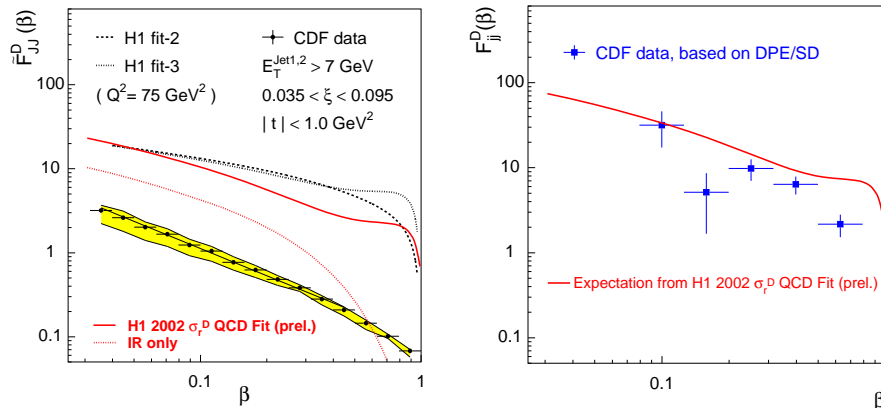


Figure 5: *Effective diffractive structure function for dijet production in  $p\bar{p}$  interactions as a function of  $\beta$ , compared to expectations of different sets of DPDFs: left, for single Pomeron exchange, right, double Pomeron exchange.*

that the range of  $\xi$  (that is  $x_p$ ) covered by the  $p\bar{p}$  measurements is beyond the range probed by the H1 data, from which the DPDFs originate. In extrapolating the H1 parameterization into this high  $\xi$  region, the Reggeon contribution is estimated to be of the order of 30 to 40%.

A lesser QCD factorization breaking is observed for diffractive dijet production in  $p\bar{p}$  events in which both baryons remain unscathed - the so called double Pomeron exchange (DPE) process [22]. Compared to expectations, the rate of dijet production is only by about factor two less abundant. This is shown in figure 5.

Effects of factorization breaking are also expected for quasi-real  $\gamma p$  interactions, due to the presence of the resolved photon component. The measurements of diffractive dijets by the H1 experiment have been compared to NLO calculations [24] based on the H1 2002 DPDFs. As shown in figure 6, a good agreement with data is obtained if the resolved photon contribution is suppressed relative to the direct contribution. The factor 0.34 that multiplies the resolved component in the calculation was motivated by the recent work of Kaidalov et al. [25].



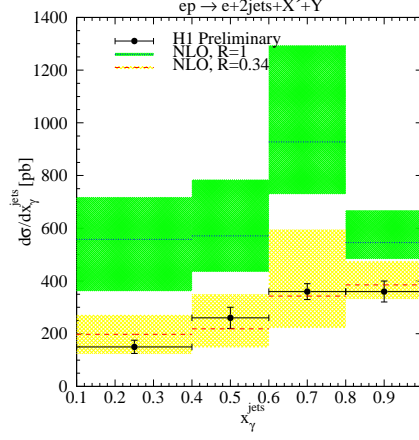


Figure 6: *Distribution of the fraction of the photon momentum involved in the hard scattering leading to two jet production,  $x_{\gamma}^{jets}$ , for the diffractive  $ep \rightarrow 2jets + X' + Y$  reaction, compared to NLO calculations without ( $R = 1$ ) or with ( $R = 0.34$ ) suppression of the resolved photon contribution.  $X'$  denotes the diffracted system accompanying the two jets, separated by a large rapidity gap from the proton or its dissociative state  $Y$ .*

## 5 Unitarity and the dipole picture

Kaidalov et al. [25] investigated what fraction of the gluon distribution in the proton leads to diffractive final states. The ratio of diffractive to inclusive dijet production cross sections as a function of  $x$  of the gluon, for different hard scattering scales and for the H1 2002 DPDFs is presented in figure 7. This ratio should be smaller than

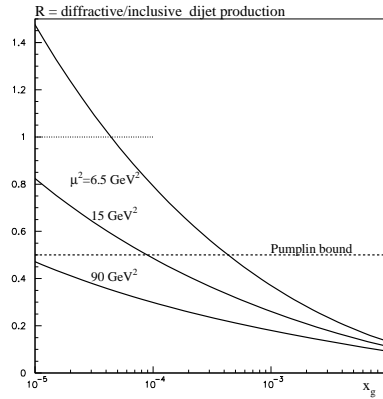


Figure 7: *The ratio of diffractive to inclusive dijet production cross section as a function of  $x$  of the gluon for different scales of the hard scattering, for the H1 2002 DPDFs. Also shown is the unitarity limit, called Pumplin bound.*

0.5 [26], while for scales  $\mu^2 = 15 \text{ GeV}^2$  this limit is exceeded for  $x = 10^{-4}$ . This

indicates that unitarity effects may already be present in diffractive scattering and may explain why the rise of diffractive scattering cross section with  $W$  is slower than expected (see section 4).

### 5.1 The dipole picture

The dynamics behind diffractive DIS can be easier understood if the process is viewed in the rest frame of the proton. The virtual photon develops a partonic fluctuations, whose lifetime is  $\tau = 1/2m_px$  [27]. At the small  $x$  typical of HERA, where  $\tau \sim 10 - 100$  fm, it is the partonic state rather than the photon that scatters off the proton. If the scattering is elastic, the final state will have the features of diffraction.

The fluctuations of the  $\gamma^*$  are described by the wave functions of the transversely and longitudinally polarized  $\gamma^*$  which are known from perturbative QCD. Small and large partonic configurations of the photon fluctuation are present. For large configurations non-perturbative effects dominate in the interaction and the treatment of this contribution is subject to modeling. For a small configuration of partons (large relative  $k_T$ ) the total interaction cross section of the created color dipole on a proton target is given by [28, 29]

$$\sigma_{q\bar{q}p} = \frac{\pi^2}{3} r^2 \alpha_S(\mu) xg(x, \mu), \quad (11)$$

$$\sigma_{q\bar{q}gp} \simeq \sigma_{ggp} = \frac{9}{4} \sigma_{q\bar{q}p}, \quad (12)$$

where  $r$  is the transverse size of the color dipole and  $\mu \sim 1/r^2$  is the scale at which the gluon distribution  $g$  of the proton is probed. The corresponding elastic cross section is obtained from the optical theorem. In this picture, the gluon dominance in diffraction results from the dynamics of perturbative QCD (see equation (12)).

Models of diffraction that follow this approach are quite successful in describing both the inclusive  $F_2$  and the diffractive  $F_2^D$  measurements, where the former are used to parameterize the dipole-proton cross section. An example taken from [30] is shown in figure 8. It is interesting to note that the two models [33, 34] which predict a relatively mild increase of  $F_2^{D(3)}$  with decreasing  $x_p$  are the ones which explicitly include effects of unitarization through saturation of cross sections for large size dipoles. The saturation scale is increasing with increasing  $W$ . The dynamical origin of this form of saturation can be derived from a new form of QCD matter, called color gluon condensate [35]. In this approach, the data suggest that the saturation scale  $Q_s > 1 \text{ GeV}^2$  for  $x < 10^{-4}$ .

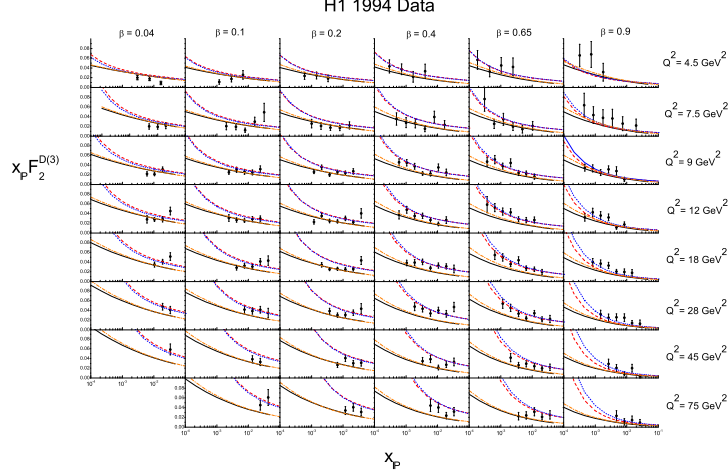


Figure 8: Comparison of dipole models from [30], McDermott, Sandapen and Shaw [31] (dashed), Forshaw, Kerney and Shaw [32] (dotted), Golec-Biernat and Wuesthoff [33] (dash-dotted) and Iancu, Itakura and Munier [34] (continuous) with  $x_P F_2^{D(3)}$  measurements.

## 6 Exclusive processes in DIS

The presence of small size  $q\bar{q}$  configurations in the photon can be tested in exclusive vector meson (VM) production as well as for deeply inelastic Compton scattering. At high energy (low  $x$ ) and in the presence of a large scale (large  $Q^2$  or heavy flavor), these reactions are expected to be driven by two-gluon exchange.

A closer look at the theory of exclusive processes in QCD shows that the two partons taking part in the exchange do not carry the same fraction of the proton momentum. That makes these processes sensitive to correlations between partons, which are encoded in the so-called generalized parton distributions, GPDs [36]. These new constructs relate in various limits to the parton distributions, form factors and orbital angular momentum distributions. The motivation behind studies of exclusive processes is to establish the region of validity of pQCD expectations and ultimately to pursue a full mapping of the proton structure, which cannot be achieved in inclusive measurements.

### 6.1 Vector meson production

The cross section for the exclusive processes is expected to rise with  $W$ , with the rate of growth increasing with the value of the hard scale. A compilation of logarithmic derivatives  $\delta = d \log \sigma(\gamma^* p) / d \log W$ , for  $\rho$  [37, 38],  $\phi$  [39, 40] and  $J/\psi$  [41, 42] exclusive production, as a function of the scale defined as  $Q^2 + M_V^2$ , where  $M_V$  is

the mass of the VM, is presented in figure 9. With decreasing transverse size of

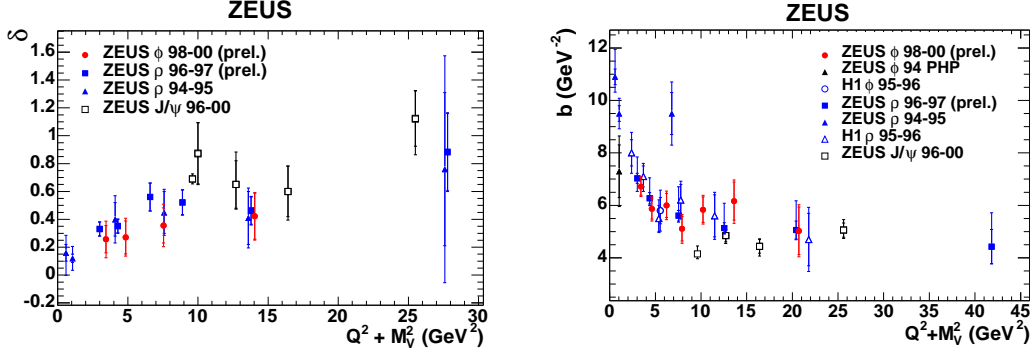


Figure 9: *Left: logarithmic derivatives  $\delta = d \log \sigma(\gamma^* p) / d \log W$  as a function of  $Q^2 + M_V^2$  for exclusive VM production. Right: exponential slope of the  $t$  distribution measured for exclusive VM production as a function of  $Q^2 + M_V^2$ .*

the dipole, the  $t$  distribution is expected to become universal, independent of the scale and of the VM. The exponential slope of the  $t$  distribution,  $b$ , reflects then the size of the proton. A compilation [37, 38, 39, 40, 41, 42] of measured  $b$  values is presented in figure 9. Around  $Q^2 + M_V^2$  of about 15 GeV<sup>2</sup> indeed the  $b$  values become universal.

Another important manifestation of the perturbative nature of exclusive processes, related to the universality of the  $t$  distribution, is that the slope,  $\alpha'_P$ , of the corresponding Regge trajectory should become small. The parameters of the effective Regge trajectory can be determined in the study of the  $W$  dependence of the differential cross section for exclusive processes at fixed  $t$ . The results obtained for exclusive vector meson production [9, 37, 39, 41, 43] are compiled in figure 10.

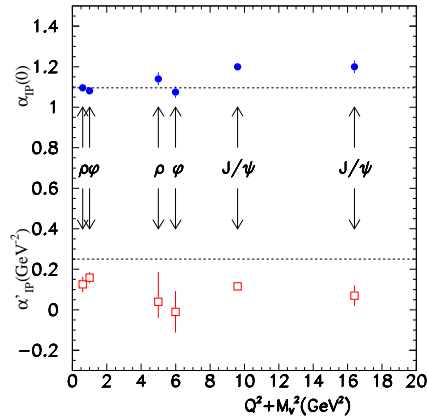


Figure 10: *Compilation of  $\alpha_P(0)$  (dots) and  $\alpha'_P$  (open squares) values, extracted in exclusive VM production, as a function of  $Q^2 + M_V^2$ .*

## 6.2 Deeply virtual Compton scattering

The deeply virtual Compton scattering (DVCS) process,  $\gamma^*p \rightarrow \gamma p$ , has been advocated as one of the exclusive processes for which theoretical calculations are free of uncertainties due to hadronic wave function uncertainties [44]. In addition, the interference of the DVCS and QED Bethe-Heitler amplitudes for prompt  $\gamma$  production is proportional to the real part of the QCD amplitude, which in turn is sensitive to GPDs.

The extraction of the DVCS cross section in  $ep$  scattering has been performed by the H1 [45] and ZEUS [46] experiments. A clear rise of the DVCS cross section with  $W$  has been observed [45, 46] as shown in figure 11. A comparison of

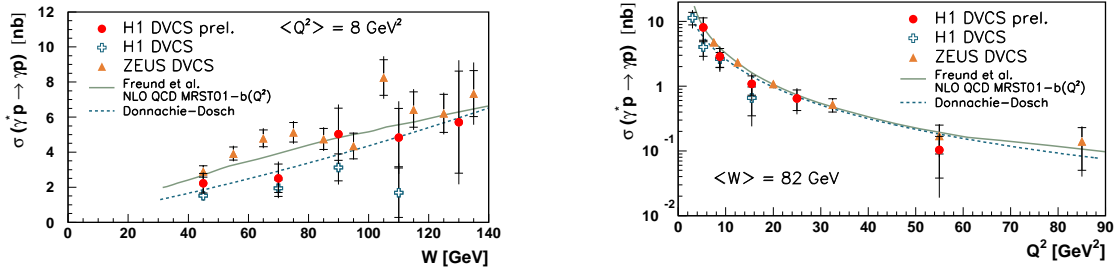


Figure 11: *The DVCS cross section,  $\sigma(\gamma^*p \rightarrow \gamma p)$  as a function of  $W$  (left) for fixed  $Q^2$  and as a function of  $Q^2$  for fixed  $W$  (right).*

the DVCS cross section dependence on  $W$  and  $Q^2$  with two approaches, one based on the dipole model [47] and the other on NLO evolution of GPDs with postulated initial conditions [48], is shown in figure 11. A good agreement with data is obtained.

## 6.3 Large $t$ exclusive processes

Diffractive production of VM or prompt  $\gamma$  at large values of  $t$  accompanied by proton dissociation, form another class of interactions which are of interest for understanding the high energy regime of pQCD. The large value of  $t$  accompanied by a large rapidity gap, suggests the applicability of the leading logarithmic BFKL dynamics [49].

The  $t$  distribution for the process  $\gamma p \rightarrow \gamma Y$  [51], where the LRG separates the photon from the dissociated proton state  $Y$  is shown in figure 12. The  $t$  distribution is well represented by calculations based on leading logarithmic BFKL approximation [49].

The BFKL approach also describes well the  $W$  dependence of the cross section for exclusive  $J/\psi$  production at large  $t$ , while expectations based on the

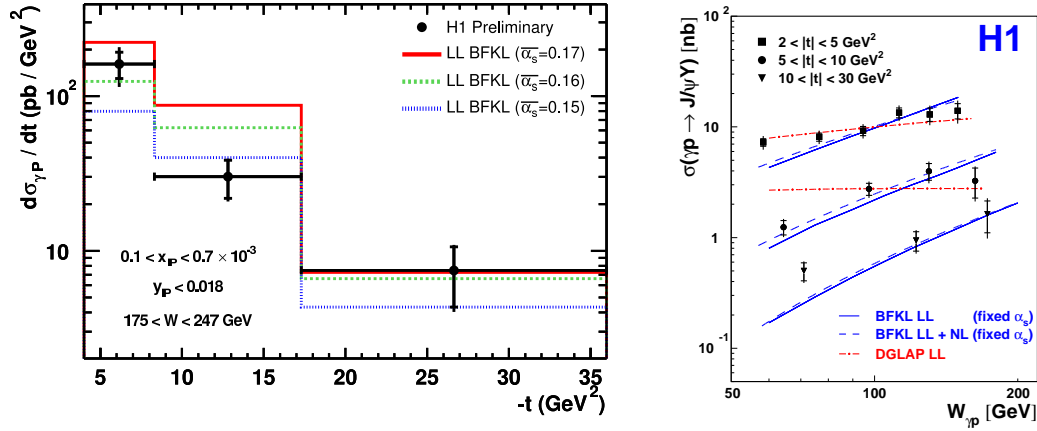


Figure 12: *Left: distribution of  $t$  at the proton vertex in the process  $\gamma p \rightarrow \gamma Y$ . The lines represent theoretical expectations based on BFKL, as described in the figure. Right:  $W$  dependence of  $\sigma(\gamma p \rightarrow J/\psi Y)$  in bins of  $t$  measured at the proton vertex. The lines represent theoretical expectations based on the BFKL or DGLAP dynamics, as described in the figure.*

leading logarithmic DGLAP dynamics fail to describe the observed dependence for  $t > 5 \text{ GeV}^2$ . This is shown in figure 12. This is yet another indication that the DGLAP dynamics, which is successfully used to describe the measurements of  $F_2$  at HERA [54, 55], may not be sufficient to describe all the features of DIS at high energy.

## 7 Exclusive states in $p\bar{p}$ interactions

The exclusive diffractive production of the Higgs boson has been proposed [56] as a potential background-free method to search for the light Higgs at LHC. A process similar to exclusive Higgs production is the exclusive  $\chi_c^0$  production, for which at the Tevatron the cross section is predicted to be about 600 nb [56]. The diagram corresponding to the proposed diffractive process is shown in figure 13. The CDF experiment [57] has searched for the exclusive process  $p\bar{p} \rightarrow p + J/\psi + \gamma + \bar{p}$  and the invariant mass of the dimuon-photon system for candidate events is shown in figure 13. Under the assumption that all found events originate from exclusive  $\chi_c^0$  production, the measured cross section was estimated to be  $50 \pm 18(\text{stat}) \pm 39(\text{syst}) \text{ pb}$ , which is far from the expected number.

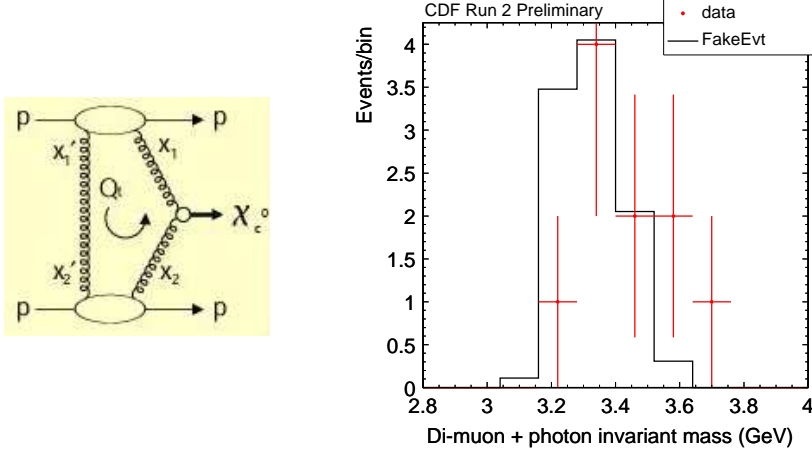


Figure 13: *Left: diagram for exclusive  $\chi_c^0$  production in  $p\bar{p}$  scattering. Right: invariant mass distribution of the candidate exclusive  $J/\psi(\mu^+\mu^-)\gamma$  system.*

## 8 Acknowledgements

I am very thankful to my colleagues from the HERA and FNAL experiments for their help in collecting the material for this talk. I would also like to acknowledge the hospitality of the Max Planck Institute in Munich, where this writeup was prepared, and the Humboldt Foundation for making my stay in Munich possible. The research was partly supported by the Israel Science Foundation.

## References

1. V. N. Gribov, JETP Lett. **41**, 667 (1961).
2. G. Ingelman and P. E. Schlein, Phys. Lett. **B152**, 256 (1985).
3. F. E. Low, Phys. Rev. **D12**, 163 (1975).
4. S. Nussinov, Phys. Rev. Lett. **34**, 1286 (1975).
5. A. Donnachie and P. V. Landshoff, Phys. Lett. **B296**, 227 (1992) [hep-ph/9209205].
6. A. Donnachie and P. V. Landshoff, Nucl. Phys. **B231**, 189 (1984).
7. K. Kang et al., hep-ph/9812429.
8. J. R. Cudell et al., Phys. Rev. D **65**, 074024 (2002).

9. J. Breitweg *et al.* [ZEUS Collaboration], Eur. Phys. J. C **14**, 213 (2000), hep-ex/9910038.
10. J. R. Forshaw and D. A. Ross, “Quantum Chromodynamics and the Pomeron,” *Cambridge University Press, 1997*.
11. J. C. Collins, Phys. Rev. **D57**, 3051 (1998) [hep-ph/9709499]; erratum Phys. Rev. **D61**, 2000 (1998).
12. A. Berera and D. E. Soper, Phys. Rev. **D53**, 6162 (1996) [hep-ph/9509239].
13. L. Trentadue and G. Veneziano, Phys. Lett. **B323**, 201 (1994).
14. H1 Collaboration, paper 089 and 090, submitted to the International Europhysics Conference on High Energy Physics, EPS03, Aachen 2003.
15. ZEUS Collaboration, paper 538, submitted to the International Europhysics Conference on High Energy Physics, EPS03, Aachen 2003.
16. S. Chekanov *et al.* [ZEUS Collaboration], submitted to Eur. Phys. J., hep-ex/0408009.
17. H1 Collaboration, paper 6-0176 submitted to the 32nd International Conference on High Energy Physics, ICHEP04, Beijing 2004.
18. H1 Collaboration, paper 113, submitted to the International Europhysics Conference on High Energy Physics, EPS03, Aachen 2003.
19. S. Chekanov *et al.* [ZEUS Collaboration], Nucl. Phys. B **672**, 3 (2003), hep-ex/0307068.
20. T. Affolder *et al.* [CDF Collaboration], Phys. Rev. Lett. **88**, 151802 (2002), hep-ex/0109025.
21. C. Adloff *et al.* [H1 Collaboration], Z. Phys. C **76**, 613 (1997), hep-ex/9708016.
22. T. Affolder *et al.* [CDF Collaboration], Phys. Rev. Lett. **85**, 4215 (2000); K. Goulianos, hep-ph/0407035.
23. H1 Collaboration, paper 87, submitted to the International Europhysics Conference on High Energy Physics, EPS03, Aachen 2003.
24. M. Klasen and G. Kramer, hep-ph/0401202.



25. A. B. Kaidalov, V. A. Khoze, A. D. Martin and M. G. Ryskin, Phys. Lett. B **567**, 61 (2003), hep-ph/0306134.
26. J. Pumplin, Phys. Rev. D **8** (1973) 2899.
27. B. L. Ioffe, V. A. Khoze and L. N. Lipatov, “Hard Processes. Vol. 1: Phenomenology, Quark Parton Model,” *Amsterdam, Netherlands: North-Holland, 1984*.
28. B. Blaettel, G. Baym, L. L. Frankfurt and M. Strikman, Phys. Rev. Lett. **70**, 896 (1993).
29. L. Frankfurt and M. Strikman, hep-ph/9907221.
30. J. R. Forshaw, R. Sandapen and G. Shaw, Phys. Lett. B **594**, 283 (2004), hep-ph/0404192.
31. M. McDermott, R. Sandapen and G. Shaw, Eur. Phys. J. C **22**, 655 (2002), hep-ph/0107224.
32. J. R. Forshaw, G. R. Kerley and G. Shaw, Nucl. Phys. A **675**, 80C (2000), hep-ph/9910251.
33. K. Golec-Biernat and M. Wusthoff, Phys. Rev. D **59**, 014017 (1999), hep-ph/9807513.
34. E. Iancu, K. Itakura and S. Munier, Phys. Lett. B **590**, 199 (2004), hep-ph/0310338.
35. L. McLerran and R. Venugopalan, Phys. Rev. **D49** 2233 (1994); Phys. Rev. **D49** 3352 (1994); Phys. Rev. **D50** 2225 (1994). For a recent review see also E. Iancu and R. Venugopalan, hep-ph/0303204.
36. D. Mueller, Fortschr. Phys. **42** 347 (1994); X. D. Ji, Phys. Rev. Lett. **78**, 610 (1997), hep-ph/9603249.
37. ZEUS Collaboration, paper 818 submitted to the 31nd International Conference on High Energy Physics, ICHEP02, Amsterdam 2002.
38. H1 Collaboration, paper 092, submitted to the International Europhysics Conference on High Energy Physics, EPS03, Aachen 2003.

39. ZEUS Collaboration, paper 6-0248 submitted to the 32nd International Conference on High Energy Physics, ICHEP04, Beijing 2004.
40. C. Adloff *et al.* [H1 Collaboration], Phys. Lett. B **483**, 360 (2000), hep-ex/0005010.
41. S. Chekanov *et al.* [ZEUS Collaboration], Nucl. Phys. B **695**, 3 (2004), hep-ex/0404008.
42. C. Adloff *et al.* [H1 Collaboration], Phys. Lett. B **483**, 23 (2000), hep-ex/0003020.
43. S. Chekanov *et al.* [ZEUS Collaboration], Eur. Phys. J. C **24**, 345 (2002), hep-ex/0201043.
44. L. L. Frankfurt, A. Freund and M. Strikman, Phys. Rev. D **58**, 114001 (1998) [Erratum-ibid. D **59**, 119901 (1999)], hep-ph/9710356.
45. H1 Collaboration, paper 115, submitted to the International Europhysics Conference on High Energy Physics, EPS03, Aachen 2003.
46. S. Chekanov *et al.* [ZEUS Collaboration], Phys. Lett. B **573**, 46 (2003), hep-ex/0305028.
47. A. Donnachie and H. G. Dosch, Phys. Lett. B **502**, 74 (2001), hep-ph/0010227.
48. A. Freund and M. McDermott, Eur. Phys. J. C **23**, 651 (2002), hep-ph/0111472.
49. L. N. Lipatov, Sov. J. Nucl. Phys. **23**, 338 (1976);
50. E. A. Kuraev, L. N. Lipatov and V. S. Fadin, Sov. Phys. JETP **45**, 199 (1977); I. I. Balitsky and L. N. Lipatov, Sov. J. Nucl. Phys. **28**, 822 (1978).
51. H1 Collaboration, paper 6-0183 submitted to the 32nd International Conference on High Energy Physics, ICHEP04, Beijing 2004.
52. A. Aktas *et al.* [H1 Collaboration], Phys. Lett. B **568**, 205 (2003), hep-ex/0306013.
53. ZEUS Collaboration, paper 549, submitted to the International Europhysics Conference on High Energy Physics, EPS03, Aachen 2003.
54. C. Adloff *et al.* [H1 Collaboration], Eur. Phys. J. C **30**, 1 (2003), hep-ex/0304003.

- 55. S. Chekanov *et al.* [ZEUS Collaboration], Phys. Rev. D **67**, 012007 (2003), hep-ex/0208023.
- 56. V. A. Khoze, A. D. Martin and M. G. Ryskin, Eur. Phys. J. C **19**, 477 (2001) [Erratum-ibid. C **20**, 599 (2001)], hep-ph/0011393.
- 57. M. Gallinaro, for the CDF Collaboration, hep-ph/0311192.